

The large-scale magnetic field of a thin accretion disk with outflows

JIAWEN LI^{1,2} AND XINWU CAO^{3,2,4}

¹*Key Laboratory for Research in Galaxies and Cosmology, Shanghai Astronomical Observatory,
Chinese Academy of Sciences, 80 Nandan Road, Shanghai, 200030, China*

²*University of Chinese Academy of Sciences, 19A Yuquan Road, 100049, Beijing, China*

³*Shanghai Astronomical Observatory, Chinese Academy of Sciences, 80 Nandan Road, Shanghai, 200030, China*

⁴*Key Laboratory of Radio Astronomy, Chinese Academy of Sciences, 210008 Nanjing, China*

(Accepted by ApJ)

ABSTRACT

The large-scale magnetic field threading an accretion disk plays an important role in launching jets/outflows. The field may probably be advected inwards by the plasma in the accretion disk from the ambient environment (interstellar medium or a companion star). It has been suggested that the external field can be efficiently dragged inwards in a thin disk with magnetic outflows. We construct a self-consistent global disk-outflow model, in which the large-scale field is formed by the advection of the external field in the disk. The outflows are accelerated by this field co-rotating with the disk, which carry away most angular momentum of the disk and make its structure significantly different from the conventional viscous disk structure. We find that the magnetic field strength in the inner region of the disk can be several orders of magnitude higher than the external field strength for a geometrically thin disk with $H/R \sim 0.1$, if the ratio of the gas to magnetic pressure $\beta_{\text{out}} \sim 10^2$ at the outer edge of the disk. The outflow velocity shows layer-like structure, i.e., it decreases with radius where it is launched. The outflow can be accelerated up to $\sim 0.2 - 0.3c$ from the inner region of the disk, and the mass loss rate in the outflows is $\sim 10 - 70\%$ of the mass accretion rate at the outer radius of the disk, which may account for the fast outflows observed in some active galactic nuclei (AGNs).

Keywords: accretion, accretion disks – magnetic fields – ISM:jets and outflows – galaxies: jets.

1. INTRODUCTION

It is widely accepted that the large scale magnetic field plays an important role in acceleration and collimation of the jets and/or outflows (see reviews of Spruit 1996, 2010; Konigl & Pudritz 2000; Pudritz et al. 2007, and the references therein). The opening configuration magnetic field is a key ingredient in both Blandford-Znajek and Blandford-Payne mechanisms (Blandford & Znajek 1977; Blandford & Payne 1982), and the kinetic power of a spinning black hole or/and the rotating accretion disk is tapped into the jets/outflows by the co-rotating large scale magnetic field. The origin of such a magnetic field threading the disk is still not well understood. It has been suggested that a dynamo working in an accretion disk can generate the required magnetic

field for launching jets/outflows (Brandenburg et al. 1995; Pudritz 1981a,1981b; Romanova et al. 1998; Armitage 1998) or the external imposed magnetic fields are transported inwards by the accretion flow (Bisnovatyi-Kogan & Ruzmaikin 1974, 1976; van Ballegoijen 1989; Lubow et al. 1994a; Spruit & Uzdensky 2005). Recent numerical simulations done by Salvesen et al. (2016) have shown that a net vertical magnetic flux is a necessary prerequisite for jet formation. This implies that a large scale magnetic field accelerating jets/outflows may probably be formed by the advection of the external weak field (e.g., the field threading the interstellar medium or the companion star in X-ray binaries) (Bisnovatyi-Kogan & Ruzmaikin 1974, 1976; van Ballegoijen 1989; Lubow et al. 1994a; Spruit & Uzdensky 2005). A steady magnetic field is formed when the inward advection of the field is counteracted by the outward field diffusion in the disk (Lubow et al. 1994a). For the turbulent plasma in an ac-

cretion disk, the magnetic diffusivity η is proportional to the turbulent viscosity ν . It is found that the magnetic Prandtl number, \mathcal{P}_m , is almost around unity, either with the rough estimation or the numerical simulations (e.g., Parker 1979; Yousef et al. 2003; Lesur & Longaretti 2009; Fromang & Stone 2009; Guan & Gammie 2009).

The advection of the field in a geometrically thin ($H/R \ll 1$) turbulent accretion disk is inefficient, because of its small radial velocity [$v_R \propto (H/R)^2$] (Lubow et al. 1994a). Several models were proposed to handle the issue of the ineffective magnetic field advection in conventional turbulent thin disks (Spruit & Uzdensky 2005; Lovelace et al. 2009; Guilet & Ogilvie 2012, 2013; Cao & Spruit 2013). It has been suggested that the magnetic flux threading the out region of the disk can be efficiently transported inwards by the comparatively fast inward moving hot corona around the disk surface, i.e., the ‘‘coronal mechanism’’ (Beckwith et al. 2009). The hot gas above the disk can be accreted inward faster than the gas inside the thin disk, which, to a certain extent, can solve the difficulty of inefficient magnetic field flux transport in the thin disk (Lovelace et al. 2009; Guilet & Ogilvie 2012, 2013). However, in the context that the jets are produced by the magnetic field transported in the hot corona, the maximum power of the jet almost less than 0.05 Eddington luminosity, which is too low to account for the strong jets ($\sim 0.1 - 1L_{\text{Edd}}$) observed in some blazars (Cao 2018). Alternatively, Cao & Spruit (2013) suggested that the most angular momentum of the disk can be removed by the magnetically driven outflows, and therefore the radial velocity of the disk is significantly higher than that of a conventional turbulent thin disk. In their work, the outflow solution is obtained with given physical properties of the gas at the disk surface as the boundary conditions. As most angular momentum of the disk is carried away by the outflows, the gas in the disk is accreting onto the black hole rapidly. Their local self-consistent accretion disk-outflow solutions show that even moderately weak fields can cause sufficient angular momentum loss via magnetic outflows to balance outward diffusion (see Cao & Spruit 2013, for the details). Their calculations are limited to the local case, and the magnetic field configuration/strength is taken as input model parameters in their calculations, however, it is known that the configuration of the advected field is determined by the whole structure of the accretion disk (mainly the radial velocity distribution) (Lubow et al. 1994a). The inclination and strength of the field at the disk surface are no longer free parameters, which are instead governed by the whole structure of the disk.

In this work, we consider the global structure of a thin accretion disk predominantly driven by the magnetic outflows, in which the outflows are calculated based on the derived global field configuration. We describe the model and numerical method in Sections 2 and 3. The results and discussion of the model calculations are given in Section 4, and the last section contains a summary of the work.

2. MODEL

For a standard thin disk, the mass accretion is driven by the turbulence in the disk, which is usually described by α -viscosity, and the disk structure can be derived analytically (Shakura & Sunyaev 1973). The disk structure will be altered in the presence of outflows, especially for strong outflows, which can carry both mass and angular momentum from the disk. Magnetically driven outflows from an accretion disk is well described by the Blandford-Payne (BP) mechanism (Blandford & Payne 1982). As discussed in Section 1, a large-scale magnetic field threading the accretion disk is a necessary ingredient of the BP mechanism, which is assumed to be formed by advection of the external weak field. A steady field is achieved when the advection is balanced with the magnetic diffusion in the disk. The magnetic field configuration/strength of the disk can be calculated with the magnetic induction equation when the disk structure (i.e., the radial velocity, density, and temperature as functions of radius) is specified (Lubow et al. 1994a). We note that the magnetic field configuration/strength in the space above the disk is determined by the field strength at the disk surface, which is a global problem, i.e., a change of local disk structure at a certain radius would alter the whole field configuration (not only the field at that radius) (see Lubow et al. 1994a, for the details). A fraction of gas at the disk surface can be centrifugally accelerated into outflows by a suitable large-scale magnetic field co-rotating with the disk. Such outflows may carry away a substantial fraction of energy and angular momentum of the disk, which makes the disk significantly different from a standard thin disk. So, the dynamical structure of the disk is coupled with the outflow solution (e.g., Ferreira & Pelletier 1993, 1995; Ferreira 1997; Ferreira et al. 2006).

In this work, we construct a steady model of the accretion disk with magnetic driven outflows. We assume a vertical weak magnetic field to be advected by a thin accretion disk to form a strong magnetic field. The outflows are accelerated by the this large-scale magnetic field co-rotating with the disk. Unlike a standard thin disk, the disk considered here is driven both by the tur-

bulence and magnetic outflows. Our model calculations consist of three parts.

1. The structure of the disk is calculated with the magnetic outflows included. Compared with the standard thin disk model, additional terms of the angular momentum and mass loss rate by the outflows should be properly included in the angular momentum and continuity equations of the disk respectively (the details will be described in Section 2.1). The properties of the outflow are to be derived with a suitable outflow model.

2. The properties of the outflow can be derived when the large-scale magnetic field configuration/strength and the rotating velocity of the disk are known with suitable boundary conditions, i.e., the density and temperature of the gas at the bottom of the outflow. The gas in the disk moves into the outflow smoothly, which is a quite complicated problem and has been studied by (Ogilvie & Livio 1998, 2001). To avoid this complexity, we assume that the outflow matches to the disk at the disk surface with a scale-height H (hereafter we refer to the place $z \sim H$ as either the bottom of the outflow or the disk surface). The gas in the outflow is driven from the disk surface, and its temperature should be the same as the disk surface temperature. The gas density of the disk varies significantly in vertical direction, and the physics of the transition region from the disk to the outflow is very complicated and quite uncertain (see Ogilvie & Livio 2001, for the detailed discussion). To avoid such complexity, we use a parameter β_s (the ratio of gas to magnetic pressure) to estimate the gas density at the disk surface H . In order to magnetically accelerate the gas at the disk surface into the outflow, the magnetic pressure should be greater than the gas pressure at the bottom of the outflow/the disk surface, i.e., $\beta_s \lesssim 1$ is required. The detailed calculations of an outflow from the disk for given magnetic field configuration/strength with boundary conditions at the disk surface will be described in Section 2.2.

3. The poloidal field advection/diffusion balance in the accretion disk is described by the magnetic induction equation. We assume a vertical weak external field to be dragged inwards by the disk extending from R_{in} to R_{out} . Above the disk, a potential field is assumed, which is a good approximation for a tenuous outflow, and is widely adopted in most previous modeling of magnetically driven outflows. The whole magnetic field configuration/strength of the disk are available by solving the induction equation as done by Lubow et al. (1994a) (see Section 2.3 for the details).

We note that three parts in our model calculations are not separable. For example, we need to know the outflow properties when calculating the disk structure,

while the calculations of the outflow requires field configuration/strength of the disk that is derived from the disk structure. So, the calculations of the model are carried out by numerical iterations.

2.1. Structure of an accretion disk with magnetically driven outflows

We consider an accretion disk with outflows centrifugally accelerated by the magnetic field lines co-rotating with the disk. A fraction of the gas is driven from the disk surface, which may remove most angular momentum of the disk, and an extra torque caused by the outflows is exerted on the disk. In this case, the accretion is driven both by the magnetic torque and the turbulence in the disk. As usual, in cylindrical coordinate, we use $\dot{M}_{\text{acc}}(R)$ to describe the mass inflow rate in the disk,

$$\dot{M}_{\text{acc}}(R) = -2\pi R \Sigma v_R, \quad (1)$$

where $\Sigma \simeq 2\rho H$ is the disk surface density, ρ , H are the mean disk density and the scale height of the disk, respectively. We note that the mass accretion rate \dot{M}_{acc} is a function of R due to the presence of outflows, which is related to the mass loss rate, \dot{m}_w , from the unit area (one surface) of the disk by the continue equation,

$$\frac{d\dot{M}_{\text{acc}}}{dR} = 4\pi R \dot{m}_w. \quad (2)$$

The momentum equation of the disk with magnetic outflows reads

$$\frac{d}{dR} (2\pi R \Sigma v_R R^2 \Omega) = \frac{d}{dR} \left(2\pi R \nu \Sigma R^2 \frac{d\Omega}{dR} \right) + 2\pi R T_m, \quad (3)$$

of which the first term in the right side describes the angular momentum transfer caused by turbulence, and the second term is due to the magnetic outflows. The radial velocity, v_R , of an accretion disk with magnetic outflows can be calculated by integrating Equation (3), which reads

$$\begin{aligned} v_R &= v_{R,\text{vis}} + v_{R,\text{m}} \\ &= -\frac{3\nu}{2R} - \frac{T_m}{\Sigma} \left[\frac{\partial}{\partial R} (R^2 \Omega) \right]^{-1} \\ &= -\frac{3\nu}{2R} - \frac{2T_m}{\Sigma R \Omega}, \end{aligned} \quad (4)$$

where the α -viscosity $\nu = \alpha c_{s,c} H$ is adopted. The approximation $d\Omega/dR \simeq -3\Omega/2R$ is used in deriving Equation (4).

For a standard thin accretion disk, its vertical structure is derived with the momentum equation by assuming the gas pressure gradient is in equilibrium with the vertical component of the gravity of the black hole

(Shakura & Sunyaev 1973). In the presence of a large-scale magnetic field, the disk structure is altered significantly especially in the strong field case, because the curved field lines exert forces on the gas of the disk both in vertical and radial directions (e.g., Ogilvie & Livio 1998, 2001; Cao & Spruit 2002). One can, in principle, solve the momentum equations in radial and vertical direction under some suitable boundary conditions to derive the magnetic field configuration (e.g., Ogilvie & Livio 2001). This is too complicated to be included in present work. A general calculation of the field configuration is described by Kippenhahn-Schlüter (KS) model (Kippenhahn & Schlüter 1957), which was established for calculating the magnetic field configuration within the solar filaments. It describes the filaments supported by the a magnetic field, which can reproduce the observations well. The KS model is valid for an isothermal plasma sheet suspended against gravity by a magnetic field, which is similar to an accretion disk vertically compressed by a magnetic field. For an isothermal accretion disk considered in this work, the KS model is applicable. Considering the cumbersome theoretical form in their model, an approximated fitting formula for KS model is given by Cao & Spruit (2002), which can reproduce the results of the KS model at a fairly good accuracy. It reads

$$R - R_0 = \frac{H}{\kappa_0 \eta_i^2} (1 - \eta_i^2 + \eta_i^2 z^2 H^{-2})^{1/2} - \frac{H}{\kappa_0 \eta_i^2} (1 - \eta_i^2)^{1/2}, \quad (5)$$

where R_0 is the radial distance of the magnetic field line footpoint, $\eta_i = \tanh(1)$, $\kappa_0 = B_z/B_{R,s}$ is the inclination of the magnetic field line with respect to horizontal at the disk surface $z = H$, and $B_{R,s}$ is the radial component of magnetic field at disk surface.

The disk is compressed in the vertical direction both by the magnetic stress (which acts like a negative pressure) and the vertical component of the gravity. With the field line shape described by Equation (5), one can solve the vertical momentum equation of an isothermal disk,

$$c_{s,s}^2 \frac{d\rho(z)}{dz} = -\rho(z)\Omega_K^2 z - \frac{B_R(z)}{4\pi} \frac{dB_R(z)}{dz}, \quad (6)$$

numerically assuming the gas to be in equilibrium vertically, and the scale-height of the disk compressed by the magnetic field is available. A fitting formula suggested by Cao & Spruit (2002)

$$\frac{H}{R} = \frac{1}{2} \left[\frac{4c_{s,c}^2}{R^2 \Omega_K^2} + \frac{(\Omega_K^2 - \Omega^2)^2}{4(1 - e^{-1/2})^2 \kappa_0^2 \Omega_K^4} \right]^{1/2} - \frac{\Omega_K^2 - \Omega^2}{4(1 - e^{-1/2}) \kappa_0 \Omega_K^2}, \quad (7)$$

which can reproduce the numerical results quite well.

The disk is rotating in a sub-Keplerian velocity, because a radial magnetic force is exerted on the gas in the disk against the gravity, i.e.,

$$R(\Omega_K^2 - \Omega^2) = \frac{B_z B_{R,s}}{2\pi \Sigma}, \quad (8)$$

which yields

$$f_\Omega \equiv \frac{\Omega}{\Omega_K} = \left[1 - \frac{2R\kappa_0}{\beta(1 + \kappa_0^2)H} \frac{c_{s,c}^2}{R^2 \Omega_K^2} \right]^{1/2}. \quad (9)$$

Using Equations (7) and (8), we obtain

$$\frac{H}{R} = \frac{c_{s,c}}{R\Omega_K} \left[1 - \frac{1}{(1 - e^{-1/2})(1 + \kappa_0^2)\beta} \right]^{1/2}, \quad (10)$$

where $\Sigma = 2\rho H$, $\kappa_0 = B_z/B_{R,s}$, and β is the ratio of the gas pressure to the magnetic pressure at mid-plane of the disk defined as

$$\beta \equiv \frac{P_{\text{gas}}}{P_{\text{mag}}} = \frac{8\pi P_{\text{gas}}}{B^2}. \quad (11)$$

The structure of the disk with magnetic outflows is available by solving a set of equations described above, provided the magnetic strength/configuration is known. We note that the magnetic torque T_m and mass loss rate m_w in outflows can be calculated with a suitable outflow model for a given magnetic field, which will be described in Sect. 2.2.

2.2. Magnetic outflows from the disk

In principle, the solution of the magnetically driven outflow is available by solving a set of MHD equations when the field strength and configuration are specified with suitable boundary conditions at the bottom of the outflow (i.e., the surface of the disk) (e.g., Cao & Spruit 1994; Cao 2014), which is an extension of the Weber-Davis model in the disk case (i.e., an axis-symmetrical rotating system). The initial Weber-Davis model was developed to explore the winds accelerated by an ideal split monopole magnetic field threading a rotating star (Weber & Davis 1967), which has a spherical symmetry. In the limit of the cold gas, i.e., the gas pressure is negligible in a magnetically driven outflow, a simple description of the outflow acceleration is available in terms of the field strength and mass loss rate (Spruit 1996; Mestel 2012). It was found that the cold Weber-Davis model applied for outflows magnetically driven from an accretion disk can reproduce the results of the numerical simulations fairly well (Anderson et al. 2005). In this work, the outflow is calculated by using the approach

suggested by [Cao & Spruit \(2013\)](#) in the frame of the cold Weber-Davis model, which is briefly summarized as follows.

The dimensionless mass loading parameter μ is defined as (see [Spruit 1996](#); [Cao & Spruit 2013](#), for the details)

$$\mu = \frac{4\pi\rho_w v_w \Omega R}{B_p^2} = \frac{4\pi\Omega R \dot{m}_w}{B_z B_p}, \quad (12)$$

where $\rho_w v_w = \dot{m}_w B_p / B_z$ is used, which is the mass flux parallel to the field line, $\Omega(R)$ is the angular velocity of the field line corotating with the disk at its footpoint, and $B_p = (B_z^2 + B_R^2)^{1/2}$ is the poloidal component of the magnetic field. For a given magnetic field line anchored in the disk at radius R rotating with the disk, the dimensionless mass loading parameter μ indicates how much mass is loaded along the field line compared with the mass accretion rate in the disk. It also determines the terminal speed of the gas accelerated by this magnetic field. The gas in the outflow will be centrifugally accelerated up to Alfvén point, at which the flow speed becomes comparable to the Alfvén speed. This is a good approximation verified by numerical magnetic outflow model calculations ([Spruit 1996](#)). Beyond the Alfvén point, the kinetic energy of the gas in the outflow $\rho v_w^2/2$ will dominate over the magnetic energy $B^2/8\pi$, and therefore further acceleration of the gas by the magnetic field is rather inefficient. The total magnetic torque T_m per unit area on the disk (including both sides) can be calculated from the mass loss rate in the outflow and the Alfvén radius

$$T_m \simeq 2\dot{m}_w R_A^2 \Omega, \quad (13)$$

where R_A is the Alfvén radius of the outflows ([Lubow et al. 1994a](#)). The solution of cold Weber-Davis model yields (see [Spruit 1996](#); [Mestel 2012](#), for detailed discussion):

$$R_A = R \left[\frac{3}{2} \left(1 + \mu^{-2/3} \right) \right]^{1/2}, \quad (14)$$

where R is the radial distance of the magnetic field line footpoint from the central black hole.

Using Equations (12) and (13) we obtain

$$T_m = \frac{3}{4\pi} R B_z B_p \mu \left(1 + \mu^{-2/3} \right). \quad (15)$$

In most of our model calculations, the accretion disk is predominantly driven by magnetic outflows, i.e., $v_{R,m} \gg v_{R,\text{vis}}$ in Equation (4). In this case,

$$v_R \simeq v_{R,m} = -\frac{2T_m}{\Sigma R \Omega}, \quad (16)$$

is a good approximation. We substitute Equations (12), (15) and (16) into Equation (2), we have

$$\frac{d \ln \dot{M}_{\text{acc}}}{d \ln R} = \frac{1}{3} (1 + \mu^{-2/3})^{-1}, \quad (17)$$

where Equation (1) is used. It indicates that the mass load parameter μ describes the relative importance of the mass loss rate in outflows with the mass accretion rate in the disk. Substituting Equation (15) into Equation (4), we have

$$v_R = -\frac{3\nu}{2R} - \frac{6c_{s,c}^2 B_z}{\beta H \Omega B_p} \mu \left(1 + \mu^{-2/3} \right), \quad (18)$$

where $c_{s,c}$ is the sound speed at the mid-plane of the disk.

We note that the dynamics of the outflow driven from the disk is described analytically, provided the field strength at the disk surface and the mass load parameter μ are specified. However, the dimensionless parameter μ can be derived only if the mass loss rate \dot{m}_w in the outflow along the field line is known (see Equation 12).

The Bernoulli equation of the gas along a field line in an isothermal outflow is

$$\frac{1}{2} v_w^2 + c_{s,s}^2 \ln \rho_w + \Psi_{\text{eff}} = \text{const}, \quad (19)$$

where $c_{s,s}$ is the sound speed (e.g., [Cao & Spruit 1994](#); [Ogilvie & Livio 1998](#)). The effective potential is

$$\Psi_{\text{eff}}(R, z) = -\frac{GM_{\text{BH}}}{(R^2 + z^2)^{1/2}} - \frac{1}{2} R^2 \Omega^2, \quad (20)$$

where Ω is the rotation rate of the footpoint at disk surface, M_{BH} is the central black hole mass. Differentiating Equation (19) along the field line, we obtain

$$(c_{s,s}^2 - v_w^2) \frac{d \ln \rho_w}{dl} + \frac{d\Psi_{\text{eff}}}{dl} = 0. \quad (21)$$

At the sonic point in the outflow, $v_w = c_{s,s}$, $d\Psi_{\text{eff}}/dl = 0$, which implies that the location of the sonic point corresponds to the maximum of the effective potential, i.e., $\Psi_{\text{eff},s} = \Psi_{\text{eff},\text{max}}$. Thus, the location of the sonic point in the outflow can be easily derived when the magnetic field configuration and the disk rotational rate are specified. Using the Bernoulli equation, one can derive the relation of the physical quantities at the bottom of the outflow with those at the sonic point as

$$\frac{1}{2} \left[1 - \left(\frac{v_{w,0}}{c_{s,s}} \right)^2 \right] + \ln \frac{v_{w,0}}{c_{s,s}} + \frac{1}{c_{s,s}^2} (\Psi_{\text{eff},s} - \Psi_{\text{eff},0}) = 0, \quad (22)$$

where the subscript “0” refers to the quantities at the bottom of the outflow, and the mass conservation $\rho_{w,s} c_{s,s} = \rho_{w,0} v_{w,0}$ is used. As $v_{w,0}/c_{s,s} \ll 1$, we have

$$\begin{aligned} \rho_{w,s} &\simeq \rho_{w,0} \exp \left(-\frac{\Psi_{\text{eff},s} - \Psi_{\text{eff},0}}{c_{s,s}^2} - \frac{1}{2} \right) \\ &\simeq \exp \left(-\frac{\Psi_{\text{eff},s} - \Psi_{\text{eff},0}}{c_{s,s}^2} \right), \end{aligned} \quad (23)$$

where $\Psi_{\text{eff},s} - \Psi_{\text{eff},0} \gg c_{s,s}^2$ is always satisfied for a magnetically driven outflow (i.e., the gas pressure is negligible in the outflow acceleration).

The mass loss rate in the outflow from unit area of an accretion disk is available,

$$\dot{m}_w \simeq \frac{B_z}{B_p} \rho_{w,0} c_s \exp\left(-\frac{\Psi_{\text{eff,max}} - \Psi_{\text{eff},0}}{c_{s,s}^2}\right), \quad (24)$$

where $\Psi_{\text{eff},s} = \Psi_{\text{eff,max}}$ because the sonic point is always located at the maximum of the effective potential (see Equation 21).

It is obvious that shape of the magnetic field line is required to calculate the effective potential along the field line, and then to derive the maximal value of the potential. The position of the sonic point z_s , and the maximal effective potential $\Psi_{\text{eff},s}$, can be calculated with this field configuration when κ_0 , and the angular velocity Ω of the disk, are known.

The temperature of the gas is crucial in calculating the mass loss rate in the outflows, which is assumed to be the same as the disk surface temperature T_s . For a thin accretion disk, the temperatures at the disk surface and the disk mid-plane are related by $\sigma T_s^4 = (4/3\tau)\sigma T_c^4$, this leads to

$$c_{s,s} = \left(\frac{4}{3\tau}\right)^{1/8} c_{s,c}, \quad (25)$$

where τ is the optical depth in vertical direction of the disk.

In order to calculate mass loss rate per unit area of the disk, \dot{m}_w , with Equation (24), we need to know the density at the base of the outflow. The density of the gas at the disk surface is quite uncertain, however, we can estimate an upper limit on the gas density at the bottom of the outflow. Within the Alfvén radius the magnetic field is strong enough to enforce the gas corotating with the field line. The magnetic pressure is assumed to be dominant over the gas pressure at the bottom of the outflow, i.e., $B_p^2/8\pi \gtrsim \rho_{w,0} c_{s,s}^2$, so the gas will move along the field lines. Otherwise, the field will be frozen in and move with the gas if $\beta_s > 1$. This implies that outflow can be launched from the disk surface only if the field strength is sufficiently strong. Let β_s be the plasma beta parameter at the base of the flow ($\beta_s \lesssim 1$), we have

$$\rho_{w,0} c_{s,s} = \beta_s \left(\frac{3\tau}{4}\right)^{1/8} \frac{B_p^2}{8\pi c_{s,c}}, \quad (26)$$

where Equation (25) is used.

Using Equations (12), (24), and (26) we find

$$\dot{m}_w = \frac{\beta_s B_z B_p}{8\pi c_{s,c}} \left(\frac{3\tau}{4}\right)^{\frac{1}{8}} \exp\left(-\frac{\Psi_{\text{eff},s} - \Psi_{\text{eff},0}}{c_{s,s}^2}\right), \quad (27)$$

where z_s is the vertical position of the sonic point. The total mass loss rate in the outflows is

$$\dot{M}_w = \int_{R_{\text{in}}}^{R_{\text{out}}} 4\pi R \dot{m}_w dR \quad (28)$$

where R_{in} and R_{out} are the inner and outer edge of the disk respectively.

For given boundary conditions of the outflow at the disk surface (i.e., temperature and density of the gas), the properties of the outflow is available with the calculations described in this section with a specified large-scale magnetic field. The magnetic torque T_m and the mass loss rate of the outflows derived here are then adopted in the calculations of the disk structure (see Section 2.1).

The terminal speed of the outflows can be derived by solving the Bernoulli equation, i.e., the equation of motion of the flows along the magnetic field lines, which describe that the total energy of the kinetic, thermal, gravitational, and a so-called ‘centrifugal energy’ is constant along the field line. We use the result derived in Spruit (1996) [Equation (74) in Sect. 7] to calculate the terminal speed of the outflows, i.e.,

$$v_\infty = R_0 \Omega \mu^{-1/3}, \quad (29)$$

where $R_0 \Omega$ is the rotational velocity of the magnetic field foot-point. The terminal speed v_∞ of the outflow is directly related to the mass load parameter μ , which indicates a fast outflow related to a low mass loading (low- μ), while a slow outflow relate to a high mass loading (high- μ).

2.3. Magnetic field configuration of the disk with outflows

As described in Section 2.2, the mass loss rate of the outflows can be calculated when the field configuration and strength are specified. With the derived mass loss rate, the torque exerted on the disk caused by the magnetic outflows is available (Eq. 4), and the disk structure can be calculated by integrating the angular momentum equation of the disk.

The evolution of poloidal magnetic field threading an accretion disk is described by the induction equation (see Equation 10 in Lubow et al. 1994a),

$$\frac{\partial}{\partial t} (R\psi) = -v_R \frac{\partial}{\partial R} (R\psi) - \frac{4\pi\eta}{c} R J_\phi, \quad (30)$$

where v_R is the radial accretion velocity, η is the magnetic diffusivity, and J_ϕ is azimuthal current density of the disk. $R\psi$ is proportional to the magnetic flux through the disk within radius R , which is a constant

along the magnetic field line. Integrating Equation (30) over the vertical direction, we have

$$\frac{\partial}{\partial t} [R\psi(R, 0)] = -v_R \frac{\partial}{\partial R} [R\psi(R, 0)] - \frac{4\pi\eta}{c} \frac{R}{2H} J_\phi^s, \quad (31)$$

where

$$J_\phi^s \equiv \int_{-H}^H J_\phi(R, z) dz.$$

The surface current density of the disk J_ϕ^s is related to the magnetic potential ψ via the Biot-Savart law,

$$\begin{aligned} \psi_d(R, 0) &= \psi(R, 0) - \psi_\infty(R, 0) \\ &= \frac{1}{c} \int_{R_{\text{in}}}^{R_{\text{out}}} \int_0^{2\pi} \frac{J_\phi^s(R') \cos\phi' d\phi' R' dR'}{(R^2 + R'^2 - 2RR' \cos\phi')^{\frac{1}{2}}}, \end{aligned} \quad (32)$$

where $\psi_d(R, 0)$ due to currents inside the accretion disk. Assuming a uniform external vertical magnetic field B_{ext} , and therefore

$$\psi_\infty(R, 0) = \frac{1}{2} B_{\text{ext}} R.$$

For a steady accretion disk-outflow system, i.e., $\partial\psi/\partial t = 0$, the advection/diffusion of the steady large scale magnetic field in the disk is described by

$$-\frac{\partial}{\partial R} [R\psi_d(R, 0)] - \frac{2\pi}{c} \frac{\alpha c_{s,c} R}{v_R} \mathcal{P}_m J_\phi^s(R) = B_{\text{ext}} R, \quad (33)$$

where $\mathcal{P}_m \equiv \eta/\nu$, is the magnetic Prandtl number. Differentiating Equation (32), we have

$$\begin{aligned} \frac{\partial}{\partial R} [R\psi_d(R, 0)] &= \\ \frac{1}{c} \int_{R_{\text{in}}}^{R_{\text{out}}} \int_0^{2\pi} \frac{(R'^2 - RR' \cos\phi') J_\phi^s(R') \cos\phi' d\phi' R' dR'}{(R^2 + R'^2 - 2RR' \cos\phi')^{\frac{3}{2}}}. \end{aligned} \quad (34)$$

Substituting this equation into Equation (33), we obtain a group of linear equations (the subscript i, j is labeled for the variables at radius R_i, R_j)

$$-\sum_{j=1}^n P_{ij} J_\phi^s(R_j) \Delta R_j - \frac{2\pi}{c} \frac{\alpha c_{s,c}(R_i) R_i}{v_R(R_i)} \mathcal{P}_m J_\phi^s(R_i) = B_{\text{ext}} R_i, \quad (35)$$

where

$$P_{ij} = \frac{1}{c} \int_0^{2\pi} \frac{(R_j - R_i \cos\phi') R_j^2}{(R_i^2 + R_j^2 - 2R_i R_j \cos\phi')^{\frac{3}{2}}} \cos\phi' d\phi',$$

$J_\phi^s(R_j)$ is the surface current density of the circular ring at radius R_j with a width of ΔR_j . The radial accretion

velocity caused both by the angular momentum transport in the outflows and turbulence is determined by equation (18),

$$v_R(R_i) = -\frac{3}{2} \frac{\alpha c_{s,c}(R_i) H_i}{R_i} - \frac{6\kappa_{0,i} \mu_i (1 + \mu_i^{-2/3}) c_{s,c}(R_i)}{\beta_i f_{\Omega,i} (1 + \kappa_{0,i}^2)^{1/2}}. \quad (36)$$

Solving the linear system (Eq. 35) with given disk structure, i.e., the radial velocity and the disk thickness, etc. We can obtain the distribution of the surface current density, and then the magnetic field potential. The magnetic potential in the space above the disk is

$$\psi_d(R, z) = \frac{1}{c} \int_{R_{\text{in}}}^{R_{\text{out}}} \int_0^{2\pi} \frac{J_\phi^s(R') \cos\phi' d\phi' R' dR'}{[R^2 + R'^2 + z^2 - 2RR' \cos\phi']^{\frac{1}{2}}}. \quad (37)$$

The poloidal magnetic field configuration can be calculated, i.e.,

$$B_R = -\frac{\partial\psi}{\partial z}, \quad (38)$$

and

$$B_z = \frac{1}{R} \frac{\partial}{\partial R} (R\psi). \quad (39)$$

2.4. Comparison with previous works

There are some similar previous works closely related with our present work. [Cao & Spruit \(1994\)](#) explored the dynamical properties of outflows accelerated by the magnetic field threading the rotating disk, in which a simplified magnetic field configuration in an analytical form is adopted to mimic a realistic field threading the disk. The temperature and density of the gas at the bottom of the outflow are taken as input model parameters. Their calculations focus on the dynamics of the gas accelerated along the field lines varying with different inclination angles. It is found that the magnetic field configuration plays a crucial role in launching outflows ([Cao & Spruit 1994](#)), though the origin of such large-scale field is not included in their work. Such a large-scale magnetic field may probably be formed through advection of external weak field threading ambient gas by the accretion disk. [Lubow et al. \(1994a\)](#) calculated how the weak external vertical magnetic field is dragged inwards by a standard thin accretion disk, in which a steady field is formed with advection and diffusion balanced. It was found that the advection of the field in a thin disk is quite inefficient due to its small radial velocity, which implies the difficulty for launching an outflow from a thin disk. Their calculations focus on the field configuration assuming the structure of the disk is not altered by the field, and the gas acceleration along the field line has not been considered in their model.

The magnetic outflow matches the disk at some place very close to the disk surface. As the vertical disk structure is complicated and it may also affect by the outflow, the vertical transition region from the disk to outflow has been studied in previous works (Ogilvie & Livio 1998, 2001). In their model calculations, the disk structure altered by the magnetic field is considered locally (for a certain radius), and the removal angular momentum from the disk by the outflow is not included. They also concluded that launching an outflow magnetically from a thin disk is difficult. In order to solve the difficulty of launching outflows from a thin accretion disk, Cao & Spruit (2013) suggested that the radial velocity is substantially increased if most angular momentum of the gas in a thin disk is removed through outflows, and therefore the weak external field can be advected inwards to form a strong field near the black hole. Their calculations were carried out for the outflow along a single field line with specified field strength and field line inclination at the disk surface as input parameters, however, the field strength/configuration are functions of radius, which are mainly determined by the whole structure of the disk (e.g., Lubow et al. 1994a). Thus, their results show that field advection in the thin disk with outflows could be very efficient locally, however, it is not sure if such mechanism works for a realistic disk (i.e., if it works at all radii of the disk). In principle, the external weak field advected by an accretion disk predominantly driven by magnetic outflows is an accretion disk-outflow coupled global problem. In this work, we present a self-consistent accretion disk-outflow solution, in which we incorporate the calculations of Cao & Spruit (2013) for local outflow structure with the global field calculated with Lubow et al. (1994a)'s method. We have not only derived the global configuration of the field advected by the disk with outflows, but also the mass loss rate and terminal speed of the outflow together with the disk structure as functions of radius. We note that a series of works have been carried out on the disk-outflow system, in which the removal of angular momentum of the gas in the disk by the magnetic outflows is properly considered. However, a rather simplified self-similar disk-outflow solution is derived in their calculations (Ferreira & Pelletier 1993, 1995; Ferreira 1997; Ferreira et al. 2006).

3. NUMERICAL METHOD

The model of an accretion disk with outflows is described in Section 2, which can be calculated numerically when the model parameters, α , β_{out} , \mathcal{P}_m , $\Theta = c_{s,c}^2/(R^2\Omega_k^2)$ (the dimensionless temperature of the disk), and τ (the optical depth of the disk) are specified. As

described in Section 2, the model calculations consist of three parts: 1. the structure of the disk with outflows; 2. the outflow solution; 3. the field configuration of the disk. The calculations of any part need the results of other two parts as input ingredients, which make the numerical calculations quite complicated. The numerical method adopted in this work is briefly described below.

1. The model calculations are started with a certain (tentative) initial radial velocity distribution $v_R(R)$ of the disk. The magnetic field advection/diffusion in the disk is described by the induction equation, which is an integral-differential equation. It can be transformed to a set of linear algebraic equations, and then be solved numerically (Lubow et al. 1994a). We consider an accretion disk extending from R_{in} to R_{out} , which is divided into n grids radially with equal width in logarithmic space ($n = 200$ is adopted in our calculations). With this tentative $v_R(R_i)$, the surface current density $J_\phi^s(R_i)$ ($i = 1, n$) is available by solving a set of n linear algebraic equations numerically (see Equation 35). The magnetic potential $R_i\psi_i$ is calculated from derived the surface current density $J_\phi^s(R_i)$ with Equation (37). Finally, derivatives of $R\psi$ give the poloidal magnetic field configuration/strength (see Equations (38) and (39)).

2. In the presence of this magnetic field, the disk is rotating at a sub-Keplerian velocity and compressed vertically. The rotating rate Ω and scale-height H/R of the disk are calculated with Equations (9) and (10), and the effective potential Ψ_{eff} along the field line can easily be calculated. Now we can calculate the mass loss rate in outflows from unit area of the disk surface \dot{m}_w as a function of radius using Equation (28), with which the mass loading parameter μ and magnetic torque T_m are derived with Equations (12) and (15) respectively.

3. The mass accretion rate of the disk with outflows is no longer constant radially. With derived mass loss rate \dot{m}_w , one can obtain the mass accretion rate as a function of radius, and then the gas density of the disk is derived. The radial velocity of the accretion disk with outflows $v_R(R)$ is obtained by calculating with Equation (18), in which the magnetic field strength/configuration obtained in step 1 are used.

The calculation is started with a tentative $v_R(R)$ distribution, and then it arrives a new radial velocity distribution for the disk. A self-consistent solution of an accretion disk-outflow system is achieved, only these two velocity distributions converge. We find that such a solution is indeed available after several iterations of step 1-3 described above.

4. RESULTS AND DISCUSSION

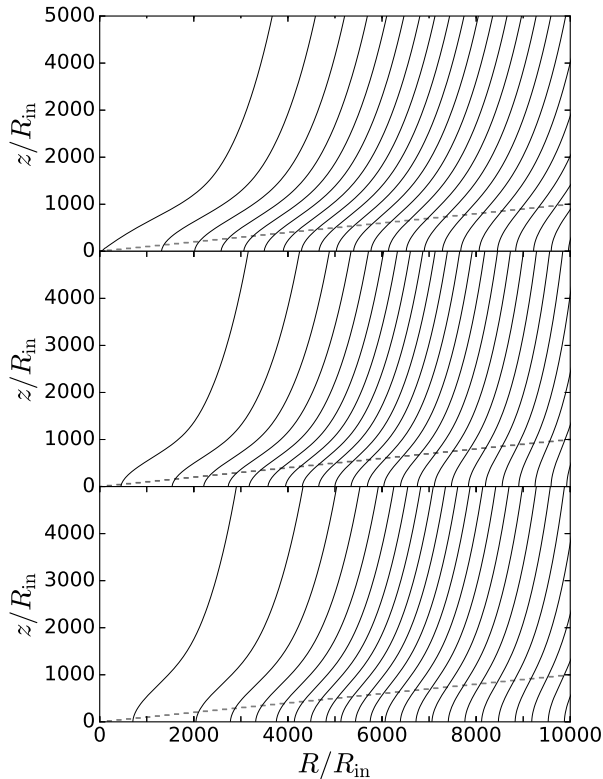


Figure 1. The poloidal magnetic field configurations of the disks with different external field strengths. The dashed lines indicate the scale height of the disk extending from R_{in} to $R_{\text{out}} = 10^4 R_{\text{in}}$. The Prandtl number $\mathcal{P}_m = 1$, and the density of the gas at the bottom of the outflow $\beta_s = 1$ are adopted in the calculations. The results calculated with $\beta_{\text{out}} = 50, 100, 200$ are plotted in three panels (from up to down) respectively. Each field line corresponds to a fixed value of $R\psi = \text{const}$, and the interval between two neighboring field lines is $\Delta R\psi(R, 0) = 0.058 R_{\text{out}} \psi_{\infty}(R_{\text{out}}, 0)$, and $\psi_{\infty}(R_{\text{out}}) = B_{\text{ext}} R_{\text{out}}/2$.

As we know that the magnetic field advected in the accretion disk is a global problem, the field strength and the inclination with respect to the disk surface is, in principle, determined by the structure of the whole disk (Lubow et al. 1994a). We study the global configuration of the large-scale poloidal magnetic field advected by the accretion disk with outflows. Most angular momentum of the disk is removed by the magnetically driven outflows. The disk is coupled with the magnetically driven outflows. Comparing with the previous works, we present self-consistent calculations of an accretion disk-outflow model (see discussion in Section 2.4). We assume a thin disk with a constant dimensionless temperature $\Theta = c_{s,c}^2/(R^2\Omega_k^2)$ independent of radius. For a conventional thin disk without magnetic outflows, $\Theta = (H/R)^2 \simeq \text{constant}$ is a good approximation for a realistic thin disk except the inner region very

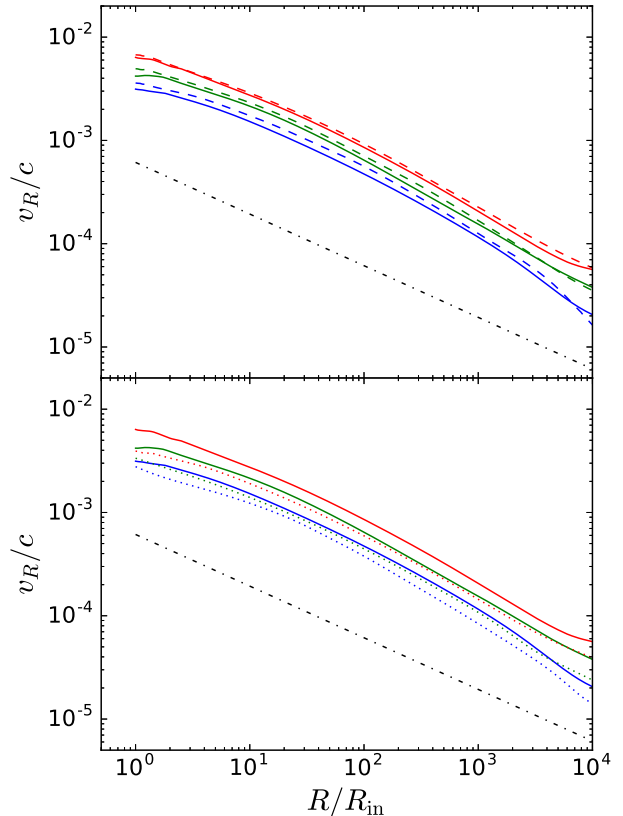


Figure 2. The radial velocity of the accretion disk varies with radius. The color lines indicate the results with different external field strengths, $\beta_{\text{out}} = 50$ (red), 100(green), and 200(blue). The solid lines correspond to the cases calculated with $\beta_s = 1$ and $\mathcal{P}_m = 1$, while the dot-dashed lines are the case of a standard thin accretion disk without outflow, as done in Lubow et al. (1994a). The dashed lines in the upper panel correspond to the results calculated with $\beta_s = 0.2$, and $\mathcal{P}_m = 1$, while the dotted lines in the lower panel are for the results calculated with $\beta_s = 1$, and $\mathcal{P}_m = 1.5$.

close to the black hole. A vertical weak external magnetic field B_{ext} is assumed to be advected by the disk, which is related to the gas pressure of the disk at the outer radius by $\beta_{\text{out}} = 8\pi P_{\text{gas}}(R_{\text{out}})/B_{\text{ext}}^2$.

In this work, the viscosity parameter $\alpha = 0.1$ is adopted in all the calculations, which is roughly consistent with that suggested by the numerical simulations (e.g., Bai & Stone 2013a, and the references therein). We note that our results are insensitive to the value of α . The temperature of the gas at the mid-plane of the disk $\Theta = 0.01$ is adopted in the calculations, which corresponds to a typical thin accretion disk with $H/R \simeq 0.1$ in the absence of magnetic field or for the weak field case. The surface temperature of the disk is lower than the temperature at the mid-plane of the disk. It is found that $c_{s,s} = (4/3\tau)^{1/8} c_{s,c}$, which indi-

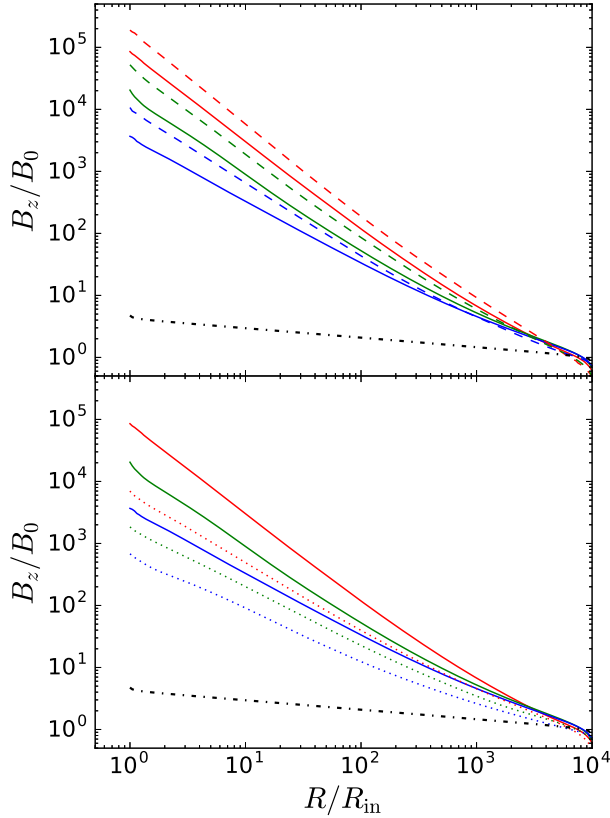


Figure 3. The vertical component of the poloidal magnetic field varies with radius. The color lines indicate the results with different external field strengths, $\beta_{\text{out}} = 50$ (red), 100 (green), and 200 (blue). The solid lines correspond to the cases calculated with $\beta_s = 1$ and $\mathcal{P}_m = 1$, while the dot-dashed lines are the case of a standard thin accretion disk without outflow, as done in [Lubow et al. \(1994a\)](#). The dashed lines in the upper panel correspond to the results calculated with $\beta_s = 0.2$, and $\mathcal{P}_m = 1$, while the dotted lines in the lower panel are for the results calculated with $\beta_s = 1$, and $\mathcal{P}_m = 1.5$.

icates the results depend on the value of τ rather weakly. We adopt a typical value $\tau = 100$ in all the calculations ([Cao & Spruit 2013](#)). The disk is assumed to extend from R_{in} to $R_{\text{out}} = 10^4 R_{\text{in}}$.

The numerical simulations show that the magnetic Prandtl number \mathcal{P}_m is always in a narrow range around unity (e.g., [Yousef et al. 2003](#); [Lesur & Longaretti 2009](#); [Fromang & Stone 2009](#); [Guan & Gammie 2009](#)). Using the numerical method described in Section. 3, we can derive a self-consistent solution of such an accretion disk-outflow system with specified values of the parameters. The large-scale magnetic field configurations of the disks with outflows are plotted in Figure 1 for different external magnetic field strength (i.e., different values of β_{out}). The magnetic Prandtl number $\mathcal{P}_m = 1$ is adopted

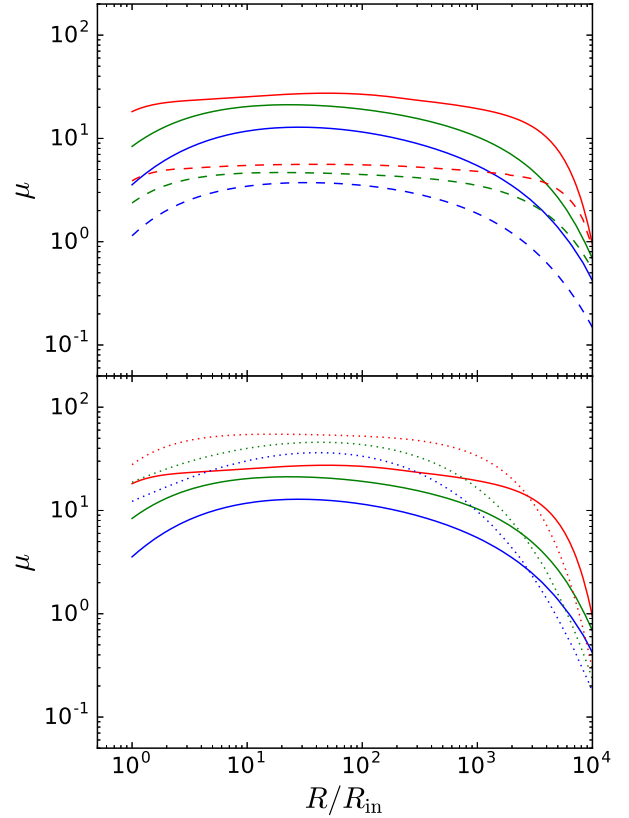


Figure 4. The mass loading parameter μ varies with radius. The color lines indicate the results with different external field strengths, $\beta_{\text{out}} = 50$ (red), 100 (green), and 200 (blue). The solid lines correspond to the cases calculated with $\beta_s = 1$ and $\mathcal{P}_m = 1$. The dashed lines in the upper panel correspond to the results calculated with $\beta_s = 0.2$, and $\mathcal{P}_m = 1$, while the dotted lines in the lower panel are for the results calculated with $\beta_s = 1$, and $\mathcal{P}_m = 1.5$.

in the calculations. It is found that the magnetic field is transported inwards and form an open configuration field threading the disk, and the field lines are significantly inclined to the disk, which is a necessary condition for launching outflows from the disk surface (e.g., [Blandford & Payne 1982](#); [Cao & Spruit 1994](#); [Cao 1997](#); [Proga 2000](#); [Cao 2012](#)). The results show that the field lines are more inclined to the disk surface for a small β_{out} , i.e., a strong external field strength case, which implies that a stronger external field is more efficient for field advection in the disk.

The magnetic torque increases with magnetic field strength and field line inclination angle, i.e., the angle of the field line with respect to the disk axis (e.g., [Cao & Spruit 1994](#); [Lubow et al. 1994b](#)). The strength of the magnetic field formed by advection increases with the external field strength, and therefore the magnetic torque due to outflows exerted on the disk increases,

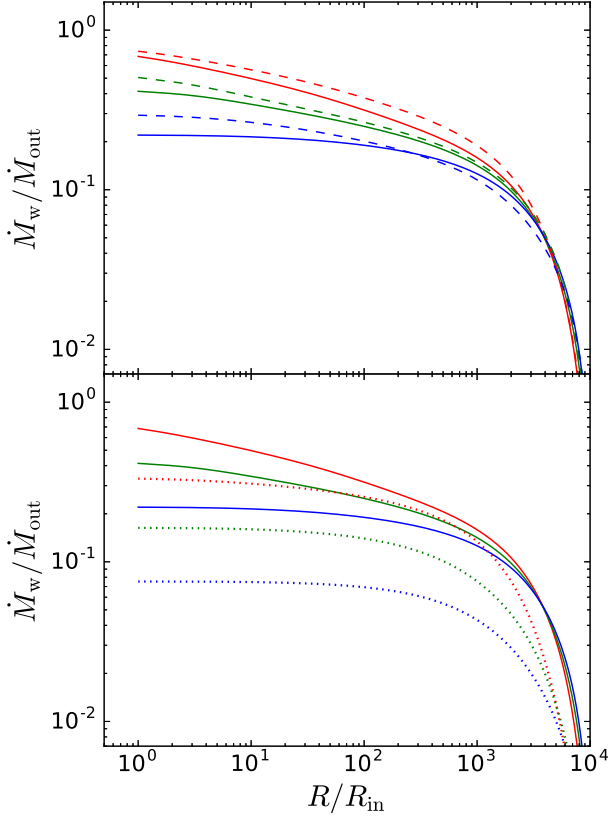


Figure 5. The mass loss rates $\dot{M}_w(R)$ in the outflows as functions of radius (integrated from the outer radius of the disk to R) with different parameter values. The color lines indicate the results with different external field strengths, $\beta_{out} = 50$ (red), 100(green), and 200(blue). The solid lines correspond to the cases calculated with $\beta_s = 1$ and $\mathcal{P}_m = 1$. The dashed lines in the upper panel correspond to the results calculated with $\beta_s = 0.2$, and $\mathcal{P}_m = 1$, while the dotted lines in the lower panel are for the results calculated with $\beta_s = 1$, and $\mathcal{P}_m = 1.5$. The mass accretion rate at the outer edge of the disk is \dot{M}_{out} .

which leads to higher radial velocities of the disk. It makes field lines inclined much to the disk surface for a stronger external field (i.e., low- β_{out}). It is well known that the acceleration of outflows is sensitive to the field line inclination at the disk surface (Blandford & Payne 1982). The field lines with large inclination angle can accelerate outflows more efficiently (e.g., Cao & Spruit 1994), which also enhances the magnetic torque.

In Figure 2, we plot the radial velocities of the accretion disks as functions of radius with different values of model parameters. It is found that the radial velocity of the disk with outflows is significantly higher than that of a conventional viscous disk. The strengths of the poloidal magnetic field dragged inwards by thin disk with outflows as functions of radius are plotted in Fig-

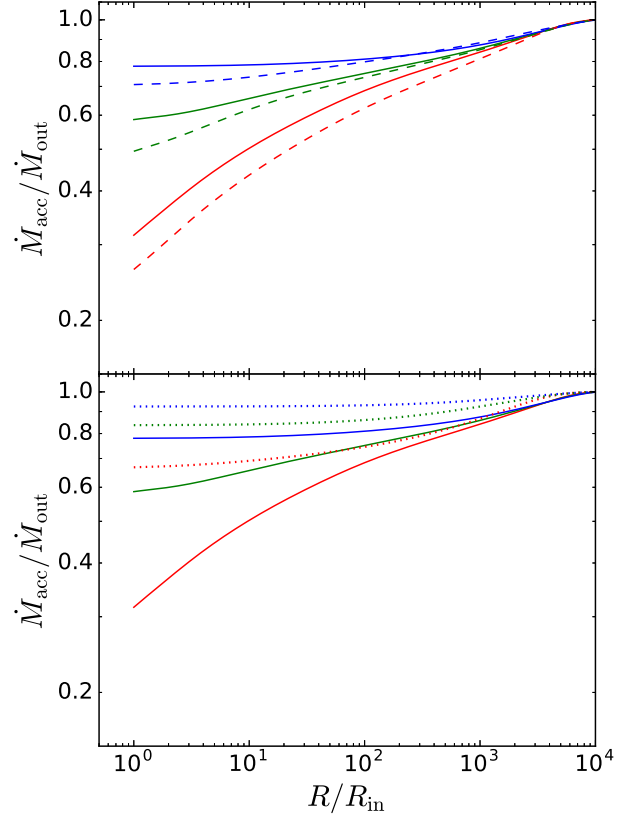


Figure 6. The mass accretion rates $\dot{M}_{acc}(R)$ as functions of radius with different parameter values. The color lines indicate the results with different external field strengths, $\beta_{out} = 50$ (red), 100(green), and 200(blue). The solid lines correspond to the cases calculated with $\beta_s = 1$ and $\mathcal{P}_m = 1$. The dashed lines in the upper panel correspond to the results calculated with $\beta_s = 0.2$, and $\mathcal{P}_m = 1$, while the dotted lines in the lower panel are for the results calculated with $\beta_s = 1$, and $\mathcal{P}_m = 1.5$. The mass accretion rate at the outer edge of the disk is \dot{M}_{out} .

ure 3 with different values of external field strength β_{out} . The magnetic field strength is significantly enhanced in the inner region of the disk, while the field advection in the conventional viscous accretion disk without outflow is very inefficient (see Figure 3), because the radial velocity of the accretion disk with outflows is substantially higher than that of a standard thin disk (see Equation 4). The amplification of the field in the disk is sensitive to the external field strength. A strong external field (low- β_{out}) leads to strong outflows, which drives the gas in the disk falls to the central black hole rapidly, and therefore the field is dragged inwards efficiently. The strength of the field in the inner region of the disk is higher for a stronger external field (i.e., a lower β_{out}).

In order to explore how the field advection in the disk is affected by the external field strength and Prandtl

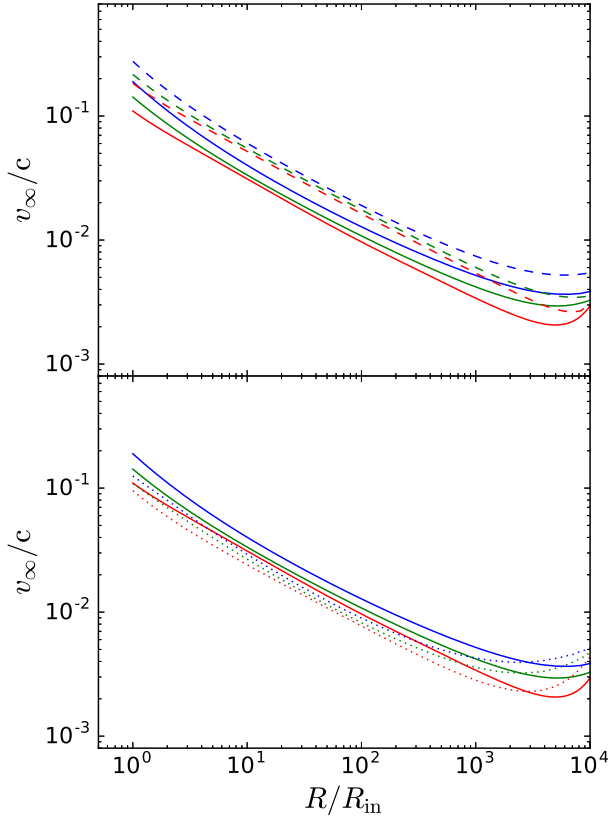


Figure 7. The terminal speeds of the outflows as functions of radius with different parameter values. The color lines indicate the results with different external field strengths, $\beta_{\text{out}} = 50$ (red), 100(green), and 200(blue). The solid lines correspond to the cases calculated with $\beta_s = 1$ and $\mathcal{P}_m = 1$. The dashed lines in the upper panel correspond to the results calculated with $\beta_s = 0.2$, and $\mathcal{P}_m = 1$, while the dotted lines in the lower panel are for the results calculated with $\beta_s = 1$, and $\mathcal{P}_m = 1.5$.

number, we also plot the results calculated with $\beta_s = 0.2$ and $\mathcal{P}_m = 1.5$ for comparison. We find that the external field can be efficiently dragged inwards with the field strength amplified several orders of magnitude in the inner region of the disk. The field advection in the standard thin accretion disk without outflow is also plotted in the same figure (see the dot-dashed lines). It is found that the field strength in the inner edge of the disk is only slightly higher than the external field strength, i.e., the field advection in a standard thin disk (Lubow et al. 1994a). We find that the field dragged inwards with outflows is obviously efficient than that in conventional turbulent thin disk. A fairly strong external field can also be formed if a low Prandtl number $\mathcal{P}_m = 1.5$ is adopted, though it is not so strong as that for $\mathcal{P}_m = 1$. In this case, more field diffusion in the disk and therefore the field is less enhanced.

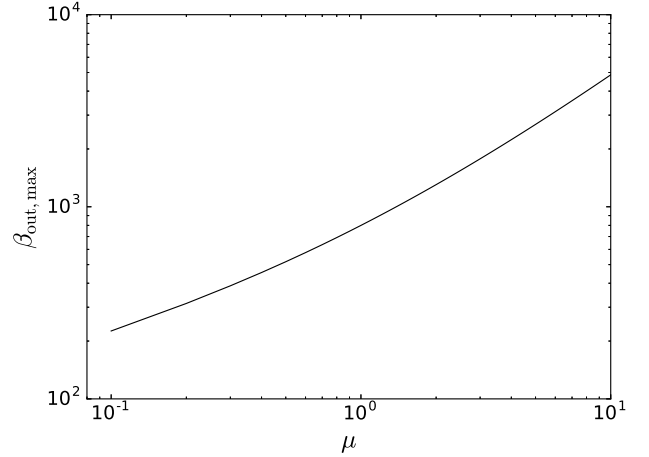


Figure 8. The minimal external field strength $\beta_{\text{out,max}}$ required at the outer edge of the disk varies with the mass load parameter μ (see Equation 40). Typical values of parameters, $\alpha = 0.1$ and $H/R = 0.1$, are adopted in the estimate.

As the gas is magnetically driven from the disk into the outflows, the mass accretion rate is no longer constant in the disk. The mass loading parameter μ varying with radius with different values of model parameters is plotted in Figure 4. The mass loss rates in the outflows integrated from the outer radius of the disk to R are plotted in Figure 5. We plot the mass accretion rates as functions of radius for different values of β_{out} in Figure 6. The total mass loss rate in the outflows is exactly the difference between the mass accretion rates at the inner and outer edges of the disk, i.e., $\dot{M}_w = \dot{M}_{\text{acc}}(R_{\text{out}}) - \dot{M}_{\text{acc}}(R_{\text{in}})$. It is found that the mass loss rate increases with decreasing gas density at the bottom of the outflow (i.e., β_s), while the mass loss rate decreases with increasing value of \mathcal{P}_m . Comparing the results in this figure with those in Figure 3, we find that much gas is driven into the outflows when the magnetic field is strong.

The terminal speeds of the outflows as functions of radius are plotted for different parameter values in Figure 7. It is found that the gas in the inner region of the disk can be accelerated to several ten percent of the light speed, while the terminal speeds of the gas from the outer region of the disk are much lower ($\sim 10^{-3} - 10^{-2} c$). Comparing this figure with Figure 6, one finds that a heavy outflow (i.e., with a high mass loss rate) is magnetically accelerated from the disk in the case of a strong external magnetic field (i.e., a small β_{out}), while its terminal speed is relatively low. In this case, the radial velocity is large, so the field is efficiently dragged inwards, the field lines are more inclined to the disk surface (see Figure 1), and the point of the maxi-

imum effective potential Ψ_{eff} along the field line is close to the disk. The gas in the disk can be relatively easier to overcome such a shallower potential barrier, which leads to a large μ (see Figure 4). A high- μ outflow usually means a heavy or dense outflow, which is too heavy to be accelerated to a high speed by the magnetic field (see the upper panel in Figure 3 and Figure 4). The terminal velocity of such an outflow is indeed low (see Figures 6 and 7). The outflow can be accelerated up to a relatively high speed with $v_{\infty} \sim 0.3c$. (see Figure 7), which is roughly consistent with the ultra-fast outflows (UFOs) detected in some luminous quasars (Tombesi et al. 2010, 2011; Gofford et al. 2013). Recent works on outflows in active galactic nuclei (AGN) (e.g. Fukumura et al. 2015, 2018; Kraemer et al. 2018) suggested that the magnetically accelerated outflow is a physically plausible approach for the outflow features observed in X-ray spectroscopic observations.

It was suggested that the highly ionized disk winds/outflows are predominantly driven by magnetic processes (i.e., magnetic pressure and/or magnetocentrifugal), and they are unlikely to be driven by the thermal or radiation force, because of their prominently large critical launching radius of winds/outflows and low ultraviolet opacity in the highly ionized winds/outflows (Miller et al. 2006a, 2016b). The outflow seems to have layer-like structure radially, i.e., the outflow have a velocity gradient along the radius of the disk surface where it is launched (see Figure 7, the terminal speeds of the outflows decrease towards the outer edge of the disk). Longterm study of the luminous Seyfert galaxy PG 1211+143 has found multiple blueshifted absorption lines (highly ionized iron) in X-ray spectra with outflow velocities of $\sim 0.06c, 0.13c$, and $0.18c$ respectively, which implies that the outflows are not moving outwards at a single velocity, but are likely to have some layer-like structure with multiple velocities (Pounds et al. 2003, 2016a,b). The terminal speeds of the gas in the outflow driven from the inner edge of the disk can be as high as $\sim 0.1 - 0.3 c$, while they decrease with increasing radius, and they are around $10^{-3} - 10^{-2} c$ for the gas from the outer region of the disk (see Figure 7), which is roughly consistent with the ultra-fast outflows (UFOs) detected in some luminous quasars. Blueshifted absorption lines in the X-ray spectra with a typical velocities of several percent of light speed are a common feature in luminous AGNs (Tombesi et al. 2011, 2010; Gofford et al. 2013).

The calculations of the outflow solutions are carried out with suitable boundary conditions (i.e., the temperature and density of the gas at the disk surface). In our work, we adopt a typical vertical optical depth of the disk $\tau = 100$ to derive the surface disk temperature.

We note that the surface temperature of the disk depends weakly with the optical depth (see Equation 25), which means the final results may not be altered much if the optical depth is calculated with a more realistic disk model. The density of gas at the disk surface is limited by the gas pressure, which should be lower than the magnetic pressure at the bottom of the outflow (i.e., $\beta_s \lesssim 1$). We calculate the cases with a lower gas density at the bottom of the outflow ($\beta_s = 0.2$). It is found that the outflows can be accelerated to a higher terminal velocity for a lower density (see Figure 7).

We note that the external field strength β_{out} is an important parameter in our model calculations. It is obvious that there is a certain external field strength, below which the accretion disk-outflow system cannot be maintained. As discussed in Section 2, a strong field of the thin disk can be formed only if the angular momentum of the gas in the disk is removed predominantly via magnetic outflows. Thus, we can roughly estimate the minimal external field strength (i.e., $\beta_{\text{out,max}}$) by assuming $v_{\text{R,m}} \sim v_{\text{R,vis}}$ in Equation (4),

$$\beta_{\text{out}} \lesssim \beta_{\text{out,max}} \sim 4\alpha^{-1}\mu \left(1 + \mu^{-2/3}\right) \left(\frac{H}{R}\right)^{-1}, \quad (40)$$

where the approximations $B_z \sim B_p$ and $\Omega \sim \Omega_k$ are adopted. We plot $\beta_{\text{out,max}}$ as a function of μ in Figure 8. We find that β_{out} is required to be lower than several hundred in order to form a strong field in a thin disk with outflows.

In our model calculations, only poloidal field is considered. However, radial field component will be sheared into azimuthal field component by differential rotation of the disk, which will trigger magnetorotational instability (MRI) (Balbus & Hawley 1991). Das et al. (2018) performed a global study on the MRI in an accretion flow with differential rotation. They found that a very strong toroidal field in the accretion flow highly suppresses the MRI-dynamo process. Salvesen et al. (2016) also found that the strong toroidal magnetic field generated in their simulation. The MRI enhances the turbulence viscosity, which is important in understanding of how turbulence arises and transports angular momentum in astrophysical accretion disks (Balbus & Hawley 1991, 1998). It was found by Bai & Stone (2013a,b) that the increasing of vertical field strength can suppress the MRI and a strong magnetocentrifugal wind is launched. In summary, such toroidal field is indeed present in the disk, and it plays an important role in the angular momentum transfer of the gas in the disk mainly through triggering turbulence, though the detailed physics still needs further investigations most probably by numerical simulations. Thus, the α -viscosity can still describe

the general features of angular momentum transfer due to turbulence in the disk fairly well even if the toroidal field is properly considered. In our model calculations, most angular momentum of the gas in the disk is removed by the outflows, which dominates over that by turbulence in the disk. This implies that our main conclusions will not be altered even if the toroidal field in the disk is considered. We note that the outflows may also be magnetically driven from the hot gas (corona) above the disk (Cao 2014), and there is indeed observational evidence that hot plasma may help launching jets in X-ray binary and AGNs (Zdziarski et al. 2011; Wu et al. 2013), which is beyond the scope of this work.

5. SUMMARY

In this work, a self-consistent global accretion disk-outflow model is constructed, in which the large-scale magnetic field is formed by the advection of the external weak field in the disk. This field is co-rotating with the accretion disk, which accelerates a fraction of the gas into outflows. The disk is driven both by turbulence and the angular momentum loss in magnetic outflows.

We find that a strong large-scale magnetic field can be formed even if an external magnetic field with moderate strength is present (β_{out} can be hundreds at the outer

edge of the disk). The field lines are inclined substantially to the disk surface, which help launching outflows. The amplification of the field in the inner region of the disk increases with the external field strength. Low gas density at the bottom of the outflows leads to strong outflows with large mass loss rate and high terminal speeds, and then strong magnetic torque, which leads to strong field enhancement in the disk.

The outflow seems to have layer-like structure radially. The terminal speed of the gas in the outflow varies from $\sim 10^{-3} - 10^{-2} c$ to $\sim 0.1 - 0.3 c$, depending on the location of the gas driven from the disk, which is roughly consistent with the UFOs detected in some luminous quasars. The further detailed comparison of the density and velocity structure of the outflow with the observations will help understanding the physics of outflow.

ACKNOWLEDGEMENTS

We thank the referee for the helpful comments/suggestions that improved the presentation of the manuscript substantially. This work is supported by the NSFC (grants 11773050 and 11833007), the CAS grant (QYZDJ-SSW-SYS023).

REFERENCES

- Anderson, J. M., Li, Z.-Y., Krasnopolsky, R., & Blandford, R. D. 2005, *ApJ*, 630, 945
- Armitage, P. J. 1998, *ApJL*, 501, L189
- Bai, X.-N., & Stone, J. M. 2013, *ApJ*, 767, 30
- Bai, X.-N., & Stone, J. M. 2013, *ApJ*, 769, 76
- Balbus, S. A., & Hawley, J. F. 1991, *ApJ*, 376, 214
- Balbus, S. A., & Hawley, J. F. 1998, *Reviews of Modern Physics*, 70, 1
- Beckwith, K., Hawley, J. F., & Krolik, J. H. 2009, *ApJ*, 707, 428
- Begelman, M. C., & Armitage, P. J. 2014, *ApJL*, 782, L18
- Bisnovatyi-Kogan, G. S., & Ruzmaikin, A. A. 1974, *Ap&SS*, 28, 45
- Bisnovatyi-Kogan, G. S., & Ruzmaikin, A. A. 1976, *Ap&SS*, 42, 401
- Blandford, R. D., & Znajek, R. L. 1977, *MNRAS*, 179, 433
- Blandford, R. D., & Payne, D. G. 1982, *MNRAS*, 199, 883
- Brandenburg, A., Nordlund, A., Stein, R. F., & Torkelsson, U. 1995, *ApJ*, 446, 741
- Cao, X. 1997, *MNRAS*, 291, 145
- Cao, X. 2012, *MNRAS*, 426, 2813
- Cao, X. 2014, *ApJ*, 783, 51
- Cao, X. 2016, *ApJ*, 817, 71
- Cao, X. 2018, *MNRAS*, 473, 4268
- Cao, X., & Spruit, H. C. 1994, *A&A*, 287, 80
- Cao, X., & Spruit, H. C. 2002, *A&A*, 385, 289
- Cao, X., & Spruit, H. C. 2013, *ApJ*, 765, 149
- Das, U., Begelman, M. C., & Lesur, G. 2018, *MNRAS*, 473, 2791
- Ferreira, J., & Pelletier, G. 1993, *A&A*, 276, 625
- Ferreira, J., & Pelletier, G. 1995, *A&A*, 295, 807
- Ferreira, J. 1997, *A&A*, 319, 340
- Ferreira, J., Petrucci, P.-O., Henri, G., Saugé, L., & Pelletier, G. 2006, *A&A*, 447, 813
- Fromang, S., & Stone, J. M. 2009, *A&A*, 507, 19
- Fukumura, K., Tombesi, F., Kazanas, D., et al. 2015, *ApJ*, 805, 17
- Fukumura, K., Kazanas, D., Shrader, C., et al. 2018, *ApJ*, 853, 40
- Gofford, J., Reeves, J. N., Tombesi, F., et al. 2013, *MNRAS*, 430, 60
- Guan, X., & Gammie, C. F. 2009, *ApJ*, 697, 1901
- Guilet, J., & Ogilvie, G. I. 2012, *MNRAS*, 424, 2097
- Guilet, J., & Ogilvie, G. I. 2013, *MNRAS*, 430, 822

- Jackson, J. D. 1998, *Classical Electrodynamics*, 3rd Edition, by John David Jackson, pp. 832. ISBN 0-471-30932-X. Wiley-VCH, July 1998., 832
- Kippenhahn R., Schlüter A., 1957, *ZA*, 43, 36
- Konigl, A., & Pudritz, R. E. 2000, *Protostars and Planets IV*, 759
- Kraemer, S. B., Tombesi, F., & Bottorff, M. C. 2018, *ApJ*, 852, 35
- Lesur, G., & Longaretti, P.-Y. 2009, *A&A*, 504, 309
- Lovelace, R. V. E., Rothstein, D. M., & Bisnovatyi-Kogan, G. S. 2009, *ApJ*, 701, 885
- Lubow, S. H., Papaloizou, J. C. B., & Pringle, J. E. 1994, *MNRAS*, 267, 235
- Lubow, S. H., Papaloizou, J. C. B., & Pringle, J. E. 1994, *MNRAS*, 268, 1010
- Mestel, L. 2012, *Stellar magnetism*, second edition. Oxford science publications (International series of monographs on physics 154)
- Miller, J. M., Raymond, J., Fabian, A., et al. 2006, *Nature*, 441, 953
- Miller, J. M., Raymond, J., Fabian, A. C., et al. 2016, *ApJL*, 821, L9
- Ogilvie, G. I., & Livio, M. 1998, *ApJ*, 499, 329
- Ogilvie, G. I., & Livio, M. 2001, *ApJ*, 553, 158
- Parker E. N., 1979, *Cosmical magnetic fields*. Chapter 17, Clarendon Press, Oxford
- Pounds, K. A., Reeves, J. N., King, A. R., et al. 2003, *MNRAS*, 345, 705
- Pounds, K., Lobban, A., Reeves, J., & Vaughan, S. 2016, *MNRAS*, 457, 2951
- Pounds, K. A., Lobban, A., Reeves, J. N., Vaughan, S., & Costa, M. 2016, *MNRAS*, 459, 4389
- Proga, D. 2000, *ApJ*, 538, 684
- Pudritz, R. E. 1981, *MNRAS*, 195, 881
- Pudritz, R. E. 1981, *MNRAS*, 195, 897
- Pudritz, R. E., Ouyed, R., Fendt, C., & Brandenburg, A. 2007, *Protostars and Planets V*, 277
- Romanova, M. M., Ustyugova, G. V., Koldoba, A. V., Chechetkin, V. M., & Lovelace, R. V. E. 1998, *ApJ*, 500, 703
- Shakura, N. I., & Sunyaev, R. A. 1973, *A&A*, 24, 337
- Spruit, H. C. 1996, arXiv:astro-ph/9602022
- Spruit, H. C. 2010, *Lecture Notes in Physics*, Berlin Springer Verlag, 794, 233
- Spruit, H. C., & Uzdensky, D. A. 2005, *ApJ*, 629, 960
- Salvesen, G., Armitage, P. J., Simon, J. B., & Begelman, M. C. 2016, *MNRAS*, 460, 3488
- Strüder, L., Briel, U., Dennerl, K., et al. 2001, *A&A*, 365, L18
- Tombesi, F., Cappi, M., Reeves, J. N., et al. 2010, *A&A*, 521, A57
- Tombesi, F., Cappi, M., Reeves, J. N., et al. 2011, *ApJ*, 742, 44
- van Ballegoijen, A. A. 1989, *Accretion Disks and Magnetic Fields in Astrophysics*, 156, 99
- Weber, E. J., & Davis, L., Jr. 1967, *ApJ*, 148, 217
- Wu, Q., Cao, X., Ho, L. C., & Wang, D.-X. 2013, *ApJ*, 770, 31
- Yousef, T. A., Brandenburg, A., & Rüdiger, G. 2003, *A&A*, 411, 321
- Zdziarski, A. A., Skinner, G. K., Pooley, G. G., & Lubiński, P. 2011, *MNRAS*, 416, 1324